A low power, high-speed miniaturized thermal modulator for comprehensive 2D gas chromatography

Sung-Jin Kim, Shaelah. M. Reidy, Bruce P. Block, Kensall D. Wise, Edward T. Zellers, and Katsuo Kurabayashi
University of Michigan, Ann Arbor, MI 48109-2125, USA
Telephone: +1–734–615–5211/ Fax: +1–734–647–3170 / E-mail: katsuo@umich.edu

ABSTRACT

In comprehensive two-dimensional gas chromatography (GC×GC), a modulator is placed at the juncture between two separation columns to focus and re-inject eluting mixture components, and thereby enhance the selectivity, sensitivity, and analyte capacity. Here, we present the design, fabrication, and testing of a two-stage microscale thermal modulator (μTM). The μTM cryogenically trap analytes eluting from the first column and thermally inject them into the second column. For this operation, each stage is periodically heated to 200 °C for 100 ms and then cooled to -50 °C for a few second. Preliminary results using a conventional capillary column interfaced to the μTM demonstrate successful modulation of a mixture of alkanes with a sensitivity enhancement as high as 24 folds.

1. INTRODUCTION

Comprehensive two-dimensional gas chromatography (GC×GC) is an analytical technique used to separate the components of complex mixtures of volatile organic compounds [1]. Unlike standard GC, which uses a single column, GC×GC couples a first column to a relatively short second column through a junction-point modulator for the enhancement of resolution and sensitivity (Fig. 1a). Mixture components separated on the first column are focused and reinjected as a series of narrow pulses onto the second column, which uses a stationary phase whose retention properties are complementary to those of the first column.

A thermal modulator (TM) is used at the interface between the two columns, providing a great degree of sensitivity enhancement [2–5]. A TM relies on low temperature to trap and focus the analytes and then reintroduces them to the second column by rapid heating. By repeating this operation in rapid succession, the vapor profile is parsed into several segments at the TM. However, conventional macro-scale TMs relying on cryogenically cooled fluids (CO_2, N_2, or air) are resource intensive [3–5] and/or demand a large amount of refrigeration work [5]. Furthermore, power dissipation for typical heating devices can be on the order of 1 kW [2, 5].

Here, we report on the design, fabrication, and preliminary testing of a μTM (Fig. 1b) that incorporates two series-coupled serpentine Pyrex-on-Si microchannels (stages) that are sequentially cooled to trap and focus vapors and then heated to desorb them. Notably, the device exhibits fast thermal response and low power consumption due to its drastically smaller size and high thermal isolation. Moreover, our μTM uses a solid-state cooling unit, thereby removing the need for consumable coolants (Fig. 1b). Preliminary results demonstrating the modulation and sensitivity enhancement of a sample mixture of hexane, heptane, and octane vapors are presented.

2. WORKING PRINCIPLE AND DESIGN

Our μTM incorporates a two-stage design (Fig. 1b) to achieve very sharp sample pulses (i.e. signal enhancement) and a low sample loss. In the two-stage modulation, analyte trapped in the first stage is thermally released into a second stage for additional focusing prior to injection into the second column. The second stage is not heated until the first stage has cooled down to a temperature sufficiently low for trapping. This alternating heating and cooling of each stage guarantees a minimal sample loss that the single-stage modulator cannot achieve [5].

The integrated on-chip micro heaters are utilized for heating the micro stage channels. The entire device is

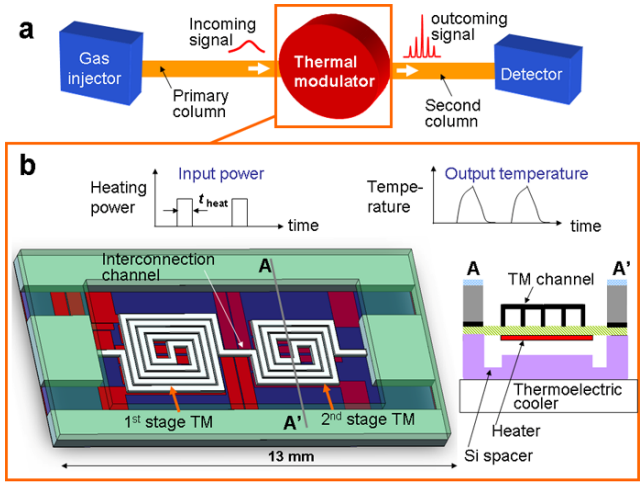

Fig. 1. Schematic of micro thermal modulator (μTM). (**a**) Comprehensive 2D gas-chromatography (GC×GC) system incorporating the μTM between two columns. (**b**) Concept of the two-stage μTM design. The μTM traps and focuses vapor species (VS) within its stage channels upon cooling and releases VS to the second column upon heating by the integrated micro heaters.

attached to a solid-state thermoelectric cooler maintained at low temperature with a 20 µm air gap. Each stage of the µTM, consisting of a meander-line microchannel, is connected by interconnection channel (IC, 1 mm length). The microchannels in each stage and the ICs have a cross section of 250 µm (width) x 140 µm (depth) and 30-µm-thick walls made from boron-doped Si. Anodically bonded Pyrex glass (100 µm thickness) is used to seal the microchannels.

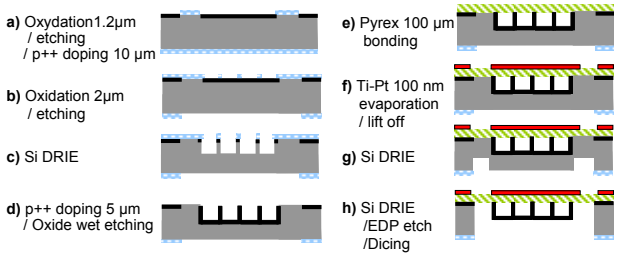

Fig. 2. Fabrication process for µTM.

3. METHODS

Microfabrication and Assembly

Figure 2 shows the microfabrication process that was employed for constructing the µTM device. (a) We first thermally grew a 1.2-µm oxide layer on the both sides of a wafer, which serve as mask layers for boron doping. Then, the front side of the wafer was photolithographically patterned. The backside was covered by photoresist, and the wafer was dipped in a buffered hydrofluoric acid (BHF) solution to selectively etch the front-side oxide layer. Afterwards, heavy boron doping was performed in a boron-diffusion furnace to define the microchannel areas. (b) The second thermal oxidation was performed to provide a diffusion barrier for the second boron doping process. Then thermal oxide layers on the both sides of the wafer were photolithographically patterned and etched in a BHF solution. (c) Microchannels (140 µm-deep and 250 µm-wide) and inlet-outlet ports (400 µm-deep and 400 µm-wide) were constructed by two-step Si deep reactive etching (DRIE). (d) The second boron doping was performed to protect the microchannels in the subsequent Si wet-etching process (step h) and the frontside oxide was removed for anodic bonding. (e) A glass wafer (Pyrex 7740, Sensors Prep Services, 100 µm thickness) was cleaned in a sulfuric-acid solution and anodically bonded to the silicon wafer. (f) Microheaters and temperature sensors were fabricated on the glass layer by the lift-off of a Ti/Pt (20 nm/100 nm in thickness) layer in an acetone solution. (g) Si DRIE was used to define the channel areas at the backside of the Si wafer. (h) The silicon portion under the glass was removed by combining Si DRIE and a wet-etching process using an ethylene-diamine-pyrocatechol solution. Finally, the wafer was diced into individual chips.

Microfabricated Si-spacers, which form a 20µm air gap between the µTM and the cooling unit, were manually aligned and bonded with a glue onto the Pyrex membrane surface of the µTM; the Si-spacers were separately fabricated by a two-step silicon DRIE process. The cooling unit is composed of a thermoelectric cooler (SP2394, Marlow industries) and a fan cooler (E1U-N7BCC-03, SundialMicro); the fan cooler facilitates heat transfer from the backside of the thermoelectric cooler. Deactivated fused silica capillaries were inserted and attached to the inlet and outlet ports of the µTM with high-temperature epoxy (Hysol 1C, Dexter Corp) to form a leak free seal, and the microchannel walls were dynamically coated with

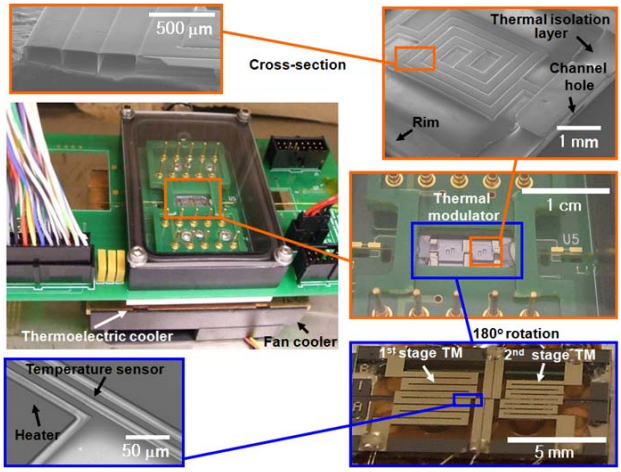

Fig. 3. Photographs of the fabricated µTM and its packaging. Each stage µTM has serpentine channels to have sufficient length at a compact area.

polydimethylsiloxane (PDMS, OV-1, Ohio Valley) from a solution (0.10 g/mL in 1:1 pentane/dichloromethane). Figure 3 shows the fabricated µTM and its packaging.

Experimental Setup

The calibration of the resistive-type temperature sensors was performed with the µTM incubated in a convection oven. To heat the µTM, a square voltage pulse was applied to the on-chip microheaters on each µTM stage using two DC power supplies (E3646A, Agilent). A custom-made computer program (C#, Microsoft) controlled the heating operation. Cooling of each stage to -55 °C was achieved by applying a constant power of 40 W (8 A and 5 V) to the thermoelectric cooler. Thus, one stage was maintained at low temperature even when the other stage was heated. Our µTM system was mounted inside a custom-made chamber on a printed circuit-board. Dry air was used in the chamber to prevent moisture condensation on the µTM surface.

For the vapor modulation, we mounted our µTM on a commercial GC system (7890A, Agilent) with a split injector (7683B, Agilent) and a flame-ionization detector. The sampling rate of the detector was 200 Hz and helium carrier gas was set to 12 cm/s. Reagent-grade test samples (Sigma-Aldrich) were injected with a split ratio of 100:1, and the injection-volume was 1 µL.

4. EXPERIMENTAL RESULTS

To characterize the thermal response of the device, we alternatively applied 100-ms square voltage pulses to each microheater (Fig. 4). When a constant voltage was applied independently to the two stages, each stage heated up and reached its maximum temperature; then it was cooled down to -55 °C by the cooling unit (Fig. 4a and 4b). Figure 5a summarizes the average heating power applied to each stage and its corresponding maximum temperature. Although the constant voltage pulse (V) was applied, the electrical resistance of the microheater (R) changes linearly with respect to temperature. This effect results in a nonlinear change of heating power (P) during the 100 ms period (i.e. $P = V^2/R$). Herewith, we define the average heating power as the time integral of $P(t)$ over the 100 ms period divided by it. As expected, the maximum temperature of each stage showed a linear relation with the average heating power. Because of the different thermal mass of each stage, it took heating powers of approximately 16 and 12 W for the first and the second stages to reach 200 °C, respectively. The cooling process from 200 to -20 °C took less than 800 ms (Fig. 5b). However, the cooling from 200 to -40 °C took more than 1.5 s for each stage. The measurements show that our device has the ability to complete the thermal modulation cycle between -55 and 200°C within a remarkably short period of time.

Figures 6a and 6b show the thermal crosstalk between the active (heater "on") and inactive (heater "off") stages. Figure 6c summarizes the temperature rise of the inactive stage (ΔT_{off_max}) by the heating (temperature rise) of the other active stage (ΔT_{on_max}), and it shows that the ΔT_{off_max} is less than 14 °C (i.e. from -55 to -36 °C) even when the temperature of the active stage reaches 200 °C. We see that the thermal crosstalk, which is defined as $\Delta T_{off\_max} / \Delta T_{on\_max} \times 100$ %, was maintained as small as 5.4% (at $T_{on\_max} = 200$ °C). Figure 6d shows the temperature response of the two stages to alternative heating and cooling with a time shift of 1 s.

Initial modulation of selected compounds was successful. Unmodulated n-heptane (Figure 7, top left) had an initial peak height of 32 pA and a full width at half-height (FWHH) of almost 5 seconds. After modulation (Figure 7, top right), peak height, at the center portion of the peak, increased to 775 pA, and peak width for the modulated slices was reduced to a FWHH of 0.34s. As seen in Figure 7 bottom, the slicing of the first-dimension peak by the modulator results in modulated peaks with various heights. The overall profile enclosing the modulated peaks should retain the shape of the unmodulated profile of the first-dimension peak. Therefore, when comparing signal enhancement, the center peak with the largest height is used, as it related to the apex of the unmodulated peak. The signal enhancement and peak width after modulation are dependent

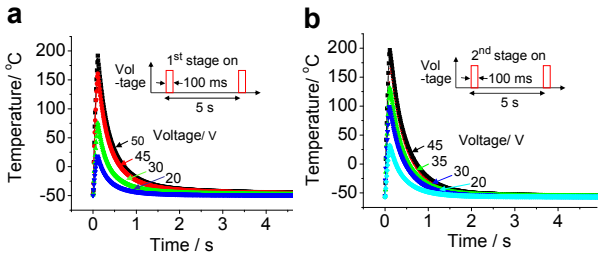

Fig. 4. Measured thermal responses for (**a**) 1st stage μTM and (**b**) 2nd stage μTM. The square heating voltage-pulse is applied in each stage with the other stage is turned off.

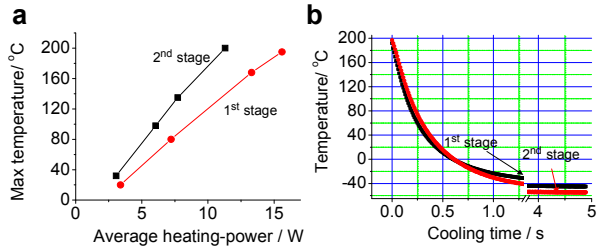

Fig. 5. Measured average heating-power and cooling response. (**a**) Average heating-power for 100 ms and its corresponding maximum temperature on each stage. (**b**) Cooling response upon turning off the microheaters on the stages.

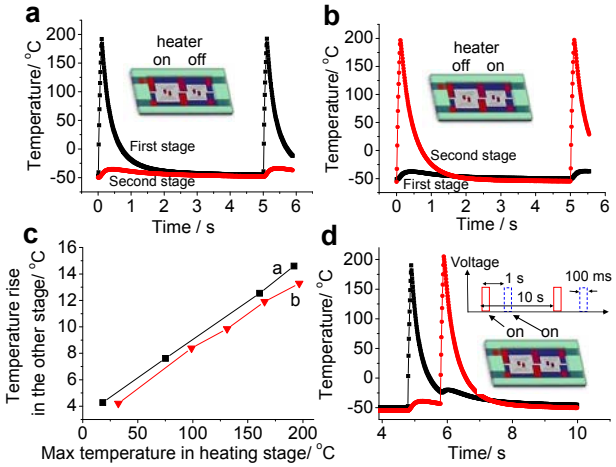

Fig. 6. Thermal crosstalk between two stages under repeated cycles. (**a** and **b**) Temperature rise of one stage by the heating of the other stage. (**c**) Maximum temperature rise on each stage. (**d**) Temperature response when both stages are alternatively turned on and off with a time shift to modulate vapor species.

on the modulation period. With a longer modulation period, there is more time for the modulator to cool back down to the initial temperature, thereby leading to better trapping efficiency.

Figure 8 shows the modulation of three straight chain alkanes. We observed some breakthrough for the most volatile hexane; however, all three have been successfully modulated. We believe that some of the broadening

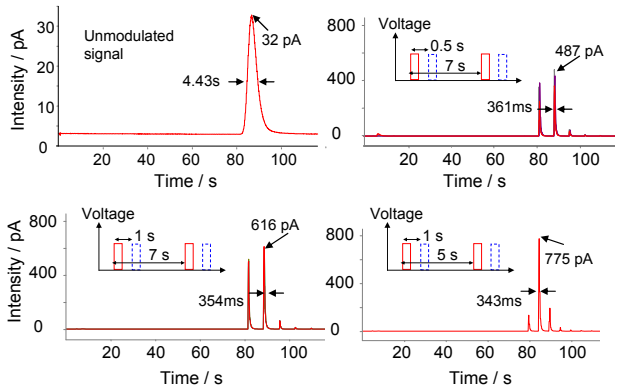

Fig. 7. Modulation of heptane vapor. Unmodulated signal represents incoming heptane to µTM, whereas modulated signals presents outcoming heptane from µTM. The focusing effect enhances the signal intensity by a factor of 15–24 and makes the signals 9–13 times sharper. The spacing between the modulated peaks corresponds to modulation period (5 or 7 s).

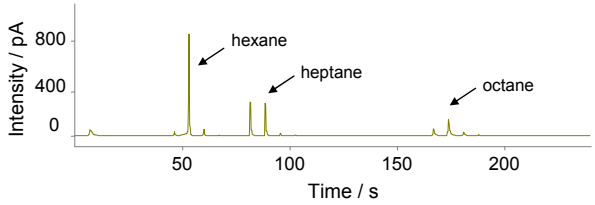

Fig. 8. Modulation for the vapor mixture of three compounds. The chromatograph is obtained using µTM (modulation period: 10s, offset: 1s).

occurring with octane is attributed to the chromatographic conditions, not to the modulator performance.

One of the major limitations of this device currently is the longer cooling time as compared to the heating time. The relatively thick (100 µm) Pyrex-membrane of the µTM causes the cooling process from 200 to -20 °C to require approximately 0.7 s (Fig. 5b). This limits the device's ability to make the modulation period shorter than 1 s. Any period shorter than this would prohibit sufficient cooling with the modulator. As a result, the breakthrough would become much more prominent for highly volatile compounds. Incorporating a thinner Pyrex-membrane in the device structure would be a promising solution to overcome this limitation.

5. CONCLUSIONS

We have developed and tested a MEMS-based µTM, designed for use in GC x GC separations of complex mixtures of volatile organic compounds. Two significant advances over the existing TMs include (1) fast thermal response at a low heating power (~10 W) where the power is two orders of magnitude smaller than that of the conventional benchtop TMs, and (2) no use of cryogenic consumables for cooling. These advantages make the use of the device attractive. Also, the thermal crosstalk between the two stages was negligible (< 9%), thereby enabling independent control of their temperatures. Ongoing work is focused on in-depth study of the separation of volatile organic compounds using our µTM, integrated in a conventional benchtop GC setup. In the near future, we will integrate the µTM with µGC columns [6–9] to develop a µGC×µGC system. The system will enable the on-site detection of complex gas-mixtures at various locations such as industrial plants, hospitals, airports, and agricultural fields.

ACKNOWLEDGEMENTS

This work was supported by NASA under the grant No. NNG-06GA89G. The authors would like to thank Katharine Beach for her advice and assistance in device fabrication, and also appreciate the help of staffs at the Lurie Nanofabrication Facility for device fabrication.

REFERENCES

[1] J. Dalluge, J. Beens and U. A. T. Brinkman, "Comprehensive two-dimensional gas chromatography: a powerful and versatile analytical tool," J. Chromatogr. A, vol. 1000, pp. 69–108, 2003.

[2] J. B. Phillips, R. B. Gaines, J. Blomberg, F. W. M. van der Wielen, J.-M. Dimandja, V. Green, J. Granger, D. Patterson, L. Racovalis, H.-J. de Geus, J. de Boer, P. Haglund, J. Lipsky, V. Sinha and E. B. Ledford, "A robust thermal modulator for comprehensive two-dimensional gas chromatography," J. High Resolut. Chromatogr., vol. 22, pp. 3–10, 1999.

[3] P. J. Marriott and R. M. Kinghorn, "Longitudinally modulated cryogenic system: a generally applicable approach to solute trapping and mobilization in gas chromatography," Anal. Chem., vol. 69, pp. 2582–2588, 1997.

[4] M. Adahchour and J. Beens, U. A. T. Brinkman, "Single-jet, single-stage cryogenic modulator for comprehensive two-dimensional gas chromatography (GC × GC)," Analyst, vol. 128, pp. 213–216, 2003.

[5] M. Libardoni, J. H. Waite and R. Sacks, "Electrically heated, air-cooled thermal modulator and at-column heating for comprehensive two-dimensional gas chromatography," Anal. Chem., vol. 77, pp. 2786–2794, 2005.

[6] S. Zampolli, I. Elmi, F. Mancarella, P. Betti, E. Dalcanale, G. C. Cardinali and M. Severi, "Real-time monitoring of sub-ppb concentrations of aromatic volatiles with a MEMS-enabled miniaturized gas-chromatograph," Sens. Actuators B, vol. 141, pp. 322–328, 2009.

[7] G. Serrano, S. M. Reidy, E. T. Zellers, "Assessing the reliability of wall-coated microfabricated gas chromatographic separation columns," Sens. Actuators B, vol. 141, pp. 217–226, 2009.

[8] M. Agah, J. A. Potkay, G. Lambertus, R. Sacks and K.D. Wise, "High-performance temperature-programmed microfabricated gas chromatography columns," J. Microelectromech. Syst., vol. 14, pp. 1039–1050, 2005.

[9] S. Reidy, G. Lambertus, J. Reece and R. Sacks, "High-performance, static-Coated silicon microfabricated columns for gas chromatography," Anal. Chem., vol. 78, pp. 2623–2630, 2006.